WATER RESOURCES RESEARCH, VOL. 35, NO. 12, PAGES 3891–3904, DECEMBER 1999

Tidal networks
1. Automatic network extraction and preliminary scaling features from digital terrain maps

Sergio Fagherazzi[1]
Dipartimento di Ingegneria Idraulica, Marittima e Geotecnica, Universitá di Padova, Padua, Italy

Annalisa Bortoluzzi[2] and William E. Dietrich
Department of Geology and Geophysics, University of California, Berkeley

Attilio Adami, Stefano Lanzoni, Marco Marani, and Andrea Rinaldo[3]
Dipartimento di Ingegneria, Idraulica, Marittima e Geotecnica, Universitá di Padova, Padua, Italy

Abstract. We propose a method of automatic extraction of the tidal channel network from topographic data of marsh and tidal flat lands that uses a combination of a threshold elevation and threshold curvature. Not only the location but also the area of the channel bed is identified. This method differs substantially from that used to identify terrestrial channel networks, and it successfully predicts all of the main channels and nearly all of the smaller tributaries of the channel networks derived from SPOT imagery of the northern Venice Lagoon. Channel network maps of Venice and other sites (Petaluma Marsh in the San Francisco Bay and Barnstable Marsh in Massachusetts) were examined for scaling properties. Because of the large width of the channels relative to a characteristic length of their drainage area, we had to develop procedures for automatically delineating channel width and then for identifying the skeleton of the channel network (the pattern connecting the loci of the channel centerlines) for box-counting analysis. Box-counting dimensions of the network skeleton proved site-dependent and showed finite-size effects. Because of the large widths we also performed a scaling analysis based on the proportions of the total channel bed area occupied by the tidal networks (i.e., a "fat" fractal analysis). This analysis showed a strong break in scaling between large and small channels. These analyses suggest that tidal channels differ significantly in their scaling relationships from terrestrial systems. In subsequent papers [*Rinaldo et al*., this issue (a), (b)] we pursue this point much further.

1. Introduction

In a tidal basin, whether it occurs within an estuary or in an open coast delimited by natural barriers, three main environments may be distinguished [e.g., *van Straaten*, 1954]: the salt marshes, the tidal flats, and the channel network. Salt marshes constitute the upper part or the more elevated portion (generally just above the mean sea level (msl)) of the tidal basin and are generally the byproduct of a complex erosional/depositional evolution. They are usually nearly flat, flooded regularly by the tide and are covered by vegetation (typically the *Spartinetum* [e.g., *Pestrong*, 1965]). The surface sediments tend to be rich in silt and clay. The second type of environment, the tidal flat, is generally at lower elevations (i.e., about or below msl) and lies between the salt marshes and the deeper tidal basin. In addition to being lower in elevation, the tidal flat is free of vegetation and becomes more sandy toward the mouth. The lack of vegetation in the tidal flat region causes tidal flows there to be more inertia-dominated as compared to the strong flow resistance encountered on the salt marsh [e.g., *Dronkers*, 1964].

The third environment is the channel network that drains the heterogeneous marshlands and tidal flat landscape. This network of channels controls to a large extent the hydrodynamics of the tidal basin and the sediment exchanges between salt marshes and tidal flats and between tidal flats and sea through the inlet. Hence tidal channel networks are of great practical importance and pose an intriguing opportunity for comparisons with terrestrial river networks, whose structure has been extensively investigated [e.g., *Rodriguez-Iturbe and Rinaldo*, 1997]. Clearly, the three components of the tidal systems are strongly interrelated, as much as hillslopes and rivers constitute an intertwined landscape system [e.g., *Montgomery and Dietrich*, 1988, 1992; *Rodriguez-Iturbe and Rinaldo*, 1997], and a detailed quantitative examination of the morphological behavior of tidal channels will contribute to an understanding of the morphological evolution of the entire tidal basin.

Many studies have described morphological characters of tidal environments. *Myrick and Leopold* [1963] applied to a small tidal estuary the hydraulic geometry concepts developed

[1]Now at Computational Science and Engineering Program, Florida State University, Tallahassee.
[2]Now at PROTECNO, Padua, Italy.
[3]Also at Ralph M. Parsons Laboratory, Massachusetts Institute of Technology, Cambridge.

Paper number 1999WR900236.
0043-1397/99/1999WR900236$09.00

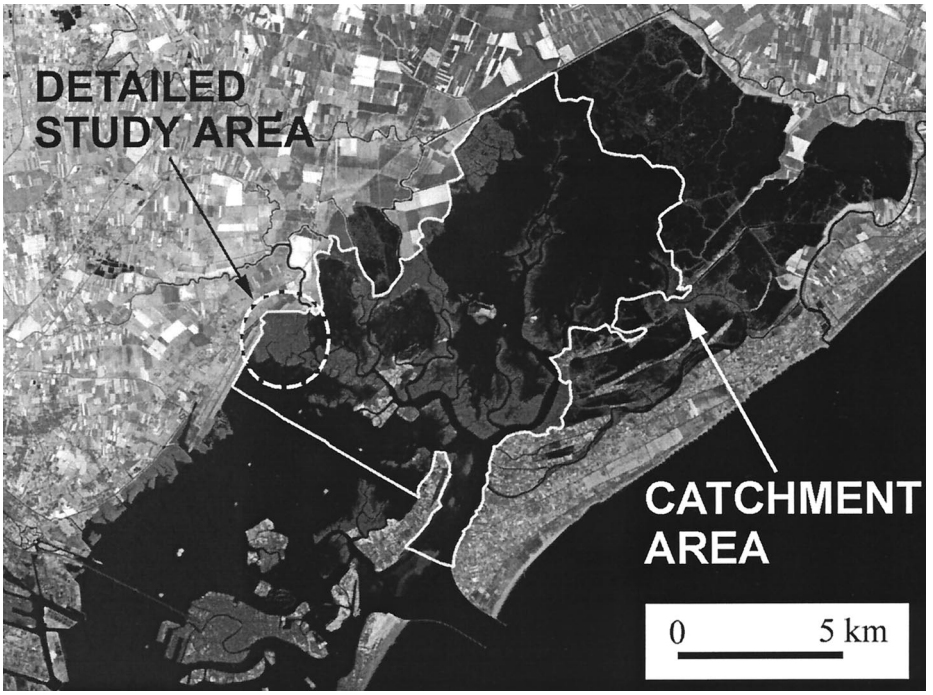

Figure 1. Satellite (SPOT 1) image of the northern part of the Venice Lagoon, chosen for its complex landforms that are only relatively perturbed by man-made interventions. The circled area represents the typical salt marsh area shown, enlarged, in Figure 2.

for fluvial networks [e.g., *Leopold and Maddock*, 1953]. They found power law relationships relating channel width and depth to an estimated maximum flow rate. Since then, many studies have investigated tidal networks and flows. Morphological descriptions of salt marshes from all over the world have been presented [e.g., *Chapman*, 1960; *Redfield*, 1972; *Pestrong*, 1965; *Ashley and Zeff*, 1988; *Allen and Pye*, 1992]. *Pestrong* [1965], *Woldenberg* [1972], *Adami et al*. [1986], and *Knighton et al*. [1992] have described tidal channel networks, mostly relying on the use of the quantitative procedures proposed by *Horton* [1945] for terrestrial rivers. As *Kirchner* [1993], *Rodriguez-Iturbe and Rinaldo* [1997], and *Rinaldo et al*. [1998] have shown, however, such properties proposed by Horton as bifurcation and length ratio of successive stream orders have values that inevitably occur for loopless networks. Hence other tools that do not have inevitable outcomes must be employed to compare tidal and terrestrial systems, and the claimed morphological resemblance found between tidal and terrestrial river networks [e.g., *Pestrong*, 1965] requires, in our view, much deeper analysis.

The complex morphology and hydrodynamics of salt marshes have been investigated by many researchers [e.g., *Boon*, 1975; *Bridges and Leeder*, 1976; *Bayliss-Smith et al*., 1979; *Healey et al*., 1981; *French and Stoddart*, 1992; *Ayles and Lapointe*, 1996]. These studies show that in marshlands the joint action of wave energy and tidal currents leads to considerable complexity in flow hydrodynamics. Marshland channels are typically, however, very stable morphologically over decadal timescales.

Extensive experimental data have been gathered on tidal networks in recent years [e.g., *Jacobson*, 1988; *Knighton et al*., 1992; *Shi et al*., 1995], particularly through large-scale field measurements and remote sensing. Here we introduce analytical tools that should provide crucial data for validation of general morphodynamic models and provide essential methods to extract information on channel networks from accurate topography. This method could prove particularly useful in analyzing high-resolution topographic data obtained from laser altimetry. Here we propose a method to identify tidal channel networks on digital elevation data sets and apply this method to a tidal system. The resulting planforms are validated and later compared with other tidal networks found in basins that differ hydrodynamically, geomorphically, and ecologically. We then analyze the planimetric development, connectivity, elongation, and topology of these tidal channel networks. We conclude that unlike river networks, tidal channel networks in different basins have widely varying scaling characteristics.

2. Study Areas

2.1. Venice Lagoon

The Venice Lagoon, an important tidal environment in Italy, occupies an area of approximately 550 km^2 and drains a freshwater-contributing catchment of approximately 1870 km^2. The rather complex runoff-producing mainland originally included [e.g., *Dorigo*, 1983] three major rivers as tributaries which were then artificially diverted outside the lagoon to prevent the filling of the lagoon with sediments. The tidal embayment is connected to the Adriatic Sea via three inlets, which throughout the centuries have been artificially modified to regulate the flow and to stabilize the depths for navigation purposes. The tidal regime is mesotidal and semidiurnal [e.g., *Gottardo and Cavazzoni*, 1981; *Comune di Venezia*, 1997]. The morphology of the lagoon is characterized by networks of channels which depart from the inlets and cut into the tidal expansion. Individual networks differ markedly in the degree and type of meandering (e.g., Figure 1). In some cases, man-made interventions are visible, as some networks have been modified by

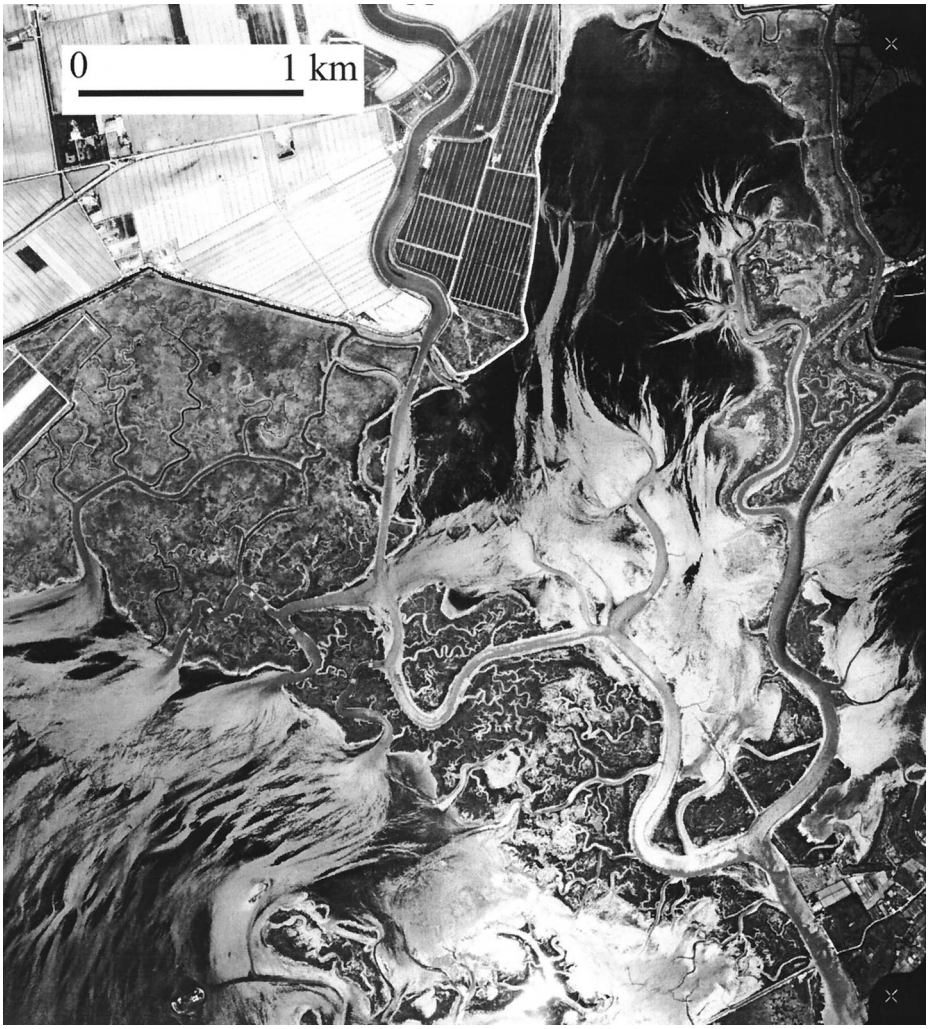

Figure 2. Aerial photograph of the Palude Pagliaga salt marsh located in the northern part of the Venice Lagoon. Note the complexity of the network forms, rather inhomogeneous within the area. The radically different degrees of irregularity of the main streams and the tributaries within the area are evident. (Courtesy of Magistrato alle Acque through Consorzio Venezia Nuova, Venice, Italy.)

land use, particularly dredging which has induced loops to form. In this paper we focus on the least disturbed area, the northern lagoon whose watershed is closed at Bocca di Lido (the Lido mouth).

The depth of channel incisions decreases from 8 to 10 m near the inlet down to less than 1 m near the most inland outer boundary of the lagoon where tidal propagation is most damped. A complex system of tidal flats and tidal marshes characterizes the areas adjacent to the channels. Given our interest in scale issues, we will extend our investigation to salt marshes and flats where the width of tidal channels is of the order of a meter, particularly in the areas located in the larger lagoonal area near the northern boundary of the lagoon, Palude Pagliaga (Figure 2). The elevation of the zones adjacent to the channels is almost constant at +0.30 m above mean sea level (ams), and these zones are flooded approximately twice a day by ordinary tides characteristic of this area. The depth of channel incisions varies from −2.00 to −0.40 m amsl. Salt marshes are bordered by tidal flats having an average elevation of approximately −0.50 m amsl. The interface between tidal flats and marshes is marked by a noticeable cliff, whose dynamic origin we will address later, roughly 0.80 m high. Freshwater inflow appears to play no role in channel morphology in this area.

Two topographic data surveys are available for the northern part of the Venice Lagoon (provided by Magistrato alle Acque di Venezia and Consorzio Venezia Nuova). The first was carried out in 1970 and is represented by 31,593 elevation points. These points are denser within the main channels than in shallow areas, where the resolution is of the order of 100 m. The second survey is ordered on a regular grid of size 20×20 m^2 and was completed in 1990 (Magistrato alle Acque di Venezia through Consorzio Venezia Nuova).

2.2. Petaluma Marsh

The investigation of tidal landforms at our second site is based on historical maps surveyed in the San Francisco Bay (California) in about 1850. Regrettably, since gold mining began here in midnineteenth century, about 95% of all tidal marshes have been filled or leveed, and no large undisturbed marshes remain. We have elected to analyze the historic maps of a tidal marshland adjacent to the Petaluma River in the northern San Francisco Bay for several reasons. First, many studies on geomorphic and hydrological processes had previ-

ously been performed on this area [see, e.g., *Leopold et al*., 1984; *Collins et al*., 1987; *Leopold et al*., 1993; *Grossinger*, 1995]. Petaluma River forms a still relatively natural marshland, the only one of its size remaining within San Francisco and San Pablo bays, and for this reason it is an object of interest in projects of restoration. The channel network of the Petaluma River, however, appears today largely modified by human activity, and no accurate and complete survey of the tidal networks of the bays has been made since the 1850s in part because of the difficulties of surveying a large unaccessible muddy and vegetated environment. However, historic maps (~1850) by the United States Coast Survey provide a large amount of high-quality information. Currently, channels range from 3 m at the inlet to 0.5 m on the marsh, and the regime is mesotidal and semidiurnal [*Collins et al*., 1987].

Although no historical data are available on surface topography, highly accurate planimetric maps of the 1850s planforms are available [*Dedrick*, 1983, also Modern and historic mapping of tidal marshlands of San Francisco Bay, California, unpublished manuscript, 1985]. The larger channels from the 1850 maps have changed little and can be readily identified on recent aerial photographs, confirming the accuracy of the earlier maps [*Grossinger*, 1995]. We digitized 1:10,000 maps to a resolution of 0.5 mm or 5 actual meters (Figure 3). Where possible, both banks of the channels were carefully digitized because the channel width of the larger channels occupies a significant portion of the catchment area, and it was therefore necessary to account for width effects in our scaling analysis. Errors involved in mapping are estimated of the order of a few meters at most; they did not affect channel network patterns.

The range of scales covered by the Petaluma tidal basin and the accuracy of the planar restitution constitute a benchmark for comparison of planar statistics and especially width detection, although obviously they cannot be used by testing our method for automatic network extraction.

2.3. Barnstable Salt Marsh

Another noteworthy tidal environment considered is a salt marsh in the Barnstable (Massachusetts, United States) estuary in the Cape Cod Bay. The enclosure in which the marsh lies occupies an area of about 55 km^2. It is bounded on the southern border by uplands, and it is protected to the north from the open sea by a sandy formation about 10 km long. The presence of a series of submerged hills and submerged deposits of freshwater peat and tree stumps are evidence of a rising sea level which was estimated to have occurred, at a rapidly decreasing rate, for the last 3000 years [*Redfield*, 1972].

The estuary communicates with the sea through an inlet, located on its eastern side, approximately 1.5 km wide. Freshwater runoff is low as no major river drains into the harbor. About half of the enclosed area is occupied by salt marsh, while sand flats occupy the open areas. The depths of the tidal channels in the flats range from tens of centimeters to about 5 m. The estuary is characterized by semidiurnal tides with a range of about 3 m at Cape Cod. The estimated water volumes in the enclosure at high and low tide are 2.8×10^7 m^3 and 2.0×10^6 m^3, respectively.

The salt marsh considered has an area of roughly 2.5 km^2, and its planar configuration (no topography was available to us) was obtained from *Redfield* [1972] by digitizing the channel structure on conventional 1:5000 maps. We digitized *Redfield*'s map to an estimated resolution of 5–10 actual meters thus preserving the details of the network patterns. As in the Petaluma case, comparative planar statistics, especially width detection, were addressed in Barnstable's case study.

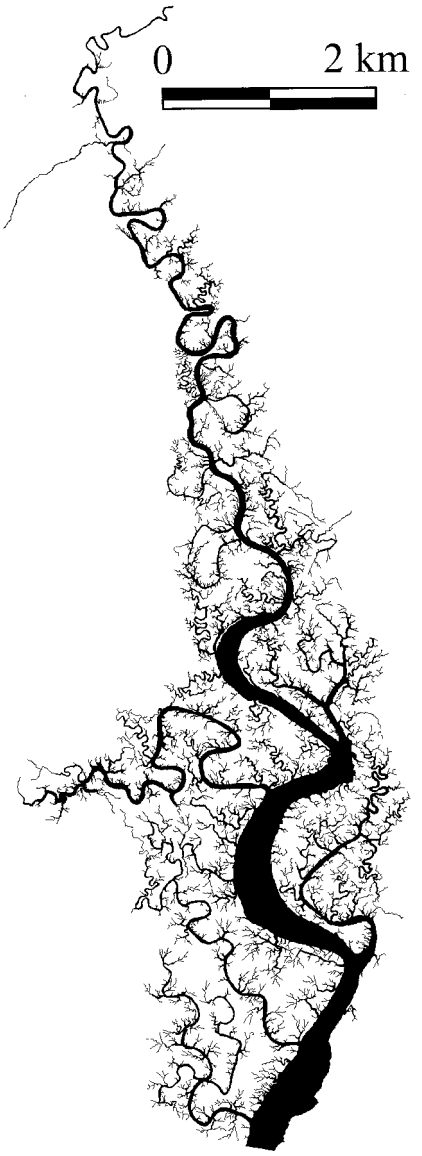

Figure 3. Planar reconstruction of the Petaluma Marsh (California) tidal network from historical maps. Here the digital set of channelized pixels is obtained with resolution 10×10 m^2.

3. Automatic Extraction of Tidal Channels

Geomorphological features of tidal networks are best examined directly through accurate topographic data, that is, from the complete set of landscape elevations $z(\mathbf{x})$ at any site (here $\mathbf{x}$ represents the vector of spatial coordinates). The elevations are expressed in meters amsl. The smallest creeks, however, are typically a meter or less in width, and unless the topographic data are of unusually high density, it is likely that such features will be missed. Especially within salt marshes, dense bathymetric data at most cover $O(10)$ m grid points. Hence, even with topographic data, high-resolution aerial photographs may be needed to quantify the finest network structure.

One first needs to grid the elevation data, which may be sparse from the survey. A regular grid of size Δx (correspond-

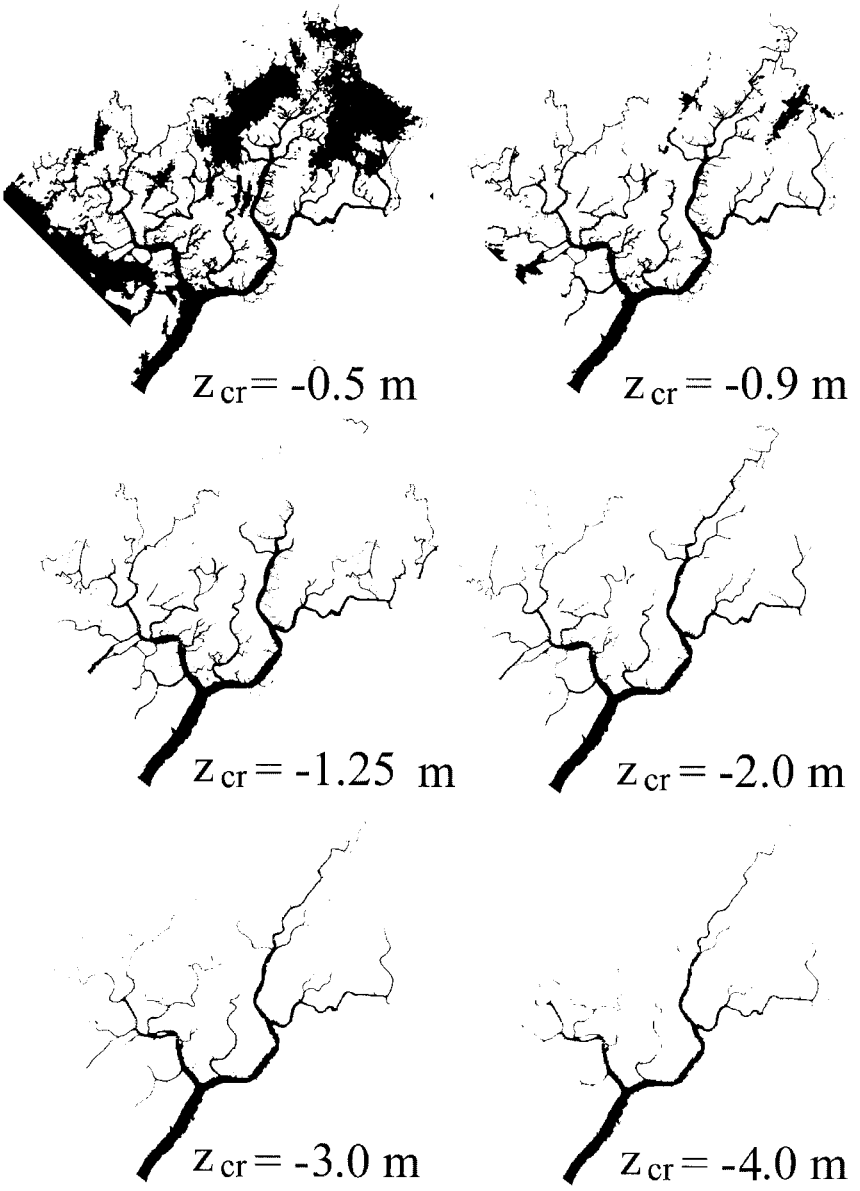

Figure 4. Network structure of the northern part of the Venice Lagoon obtained through the elevation threshold criterion for various values of the threshold: $z_{cr} = -0.5$ m; $z_{cr} = -0.9$ m; $z_{cr} = -1.25$ m; $z_{cr} = -2.0$ m; $z_{cr} = -3.0$ m; and $z_{cr} = -4.0$ m. Notice that the main structure is resilient to the value of threshold, while the fine structure is much affected by low values.

ing to the spacing of topographic measures) is used thus defining pixels whose centroid **x** is assigned the reference elevation $z(\mathbf{x})$. Various methodologies can be employed, and for the northern Venice Lagoon test site both kriging and spline interpolators were used (R. Rosselli, Consorzio Venezia Nuova, personal communication, 1997) to yield a regular spacing from sparse data obtained by stereorestitution for marshlands and accurate cross-section topographic measurements for channels. Ground validation through traditional survey have also been performed. Also, in order to evaluate our proposed model, SPOT 1 multispectral data of the Venice Lagoon taken on May 4, 1989, with resolution 20×20 m^2 were used to map the channel network. Channels were identified based on tuning of the brightness and the contrast of the gray scale of the three bands.

The pixels, like tiles, cover the set of topographic data field as customary in digital terrain maps (DTMs) [e.g., *Montgomery and Dietrich*, 1992], and those attributed to the tidal network are shown as solid (Figure 4). In order to reconstruct the network patterns, the planar domain containing measured bathymetric data (i.e., landscape elevations $z(\mathbf{x})$) is partitioned into two subsets specifying the points belonging to channels and the points belonging to flats and marshes.

One method for estimating channel locations is to assume that low spots must be channels. By selecting various critical elevations relative to mean sea level, one can delineate those lower grid points that possibly locate channels and compare the results with the observed channel network. Therefore let z_{cr} be the elevation of a reference horizontal plane, chosen below the mean sea level. We assign to the "channel" subset all

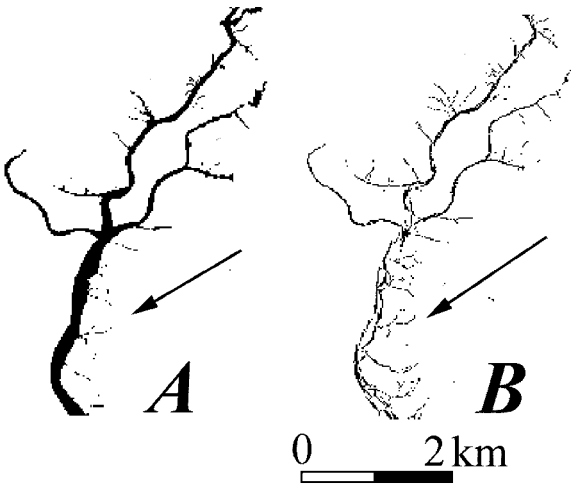

Figure 5. An enlarged detail of the comparison between networks extracted through the elevation and the curvature threshold criteria: (a) $z_{cr} = -1.3$ m and (b) $\nabla^2 z_{cr} = 0.001$ m^{-1}.

the experimental points whose elevations $z(\mathbf{x})$ are less than z_{cr} (i.e., $z(\mathbf{x}) \leq z_{cr}$). Otherwise, the pixel is assigned to the tidal flat subset. Networks obtained by choosing various values of z_{cr} are shown in Figure 4. Notice that for unsuitably low values of the threshold the tips of the extracted networks are artificially expanded into flat areas in a phenomenon similar to the feathering observed in river networks [*Montgomery and Foufoula-Georgiou*, 1993].

It clearly appears that although this method is able to capture the general channel structure, nevertheless, it fails to characterize properly important connectivity properties at the fine and very fine scales, especially in the lower zones of the basin (see Figure 5a). If the chosen threshold z_{cr} is too low, in fact, the method is unable to identify the finer and more elevated branches of the network. However, too large a threshold value will incorrectly include portions of tidal flats in the channel subset.

An alternative procedure might be to follow that used in terrestrial environments of relating channel initiation to local slope and drainage area. In tidal systems, however, it is the water surface slope, not the very flat tidal marsh slope, that drives erosion processes. Hence this approach will not apply here. With sufficient topographic resolution, however, the local curvature associated with the elevation field across the tidal flat to the channel bed should help indicate channel location. Figure 6 shows a map of channel locations based on various critical curvatures, $\nabla^2 z_{cr}$, as for the identification of the channelized portion of a fluvial DTM [*Howard*, 1994]. Basically, the method takes into account the fact that both small channels and the outer lateral portions of main channels (with the possible exception of cliffs at the boundaries of eroding marshlands) exhibit a marked topographic concavity that is detected by suitable topographic resolutions. In Figure 5b the map most closely matching the observed case based on a curvature threshold is compared with that computed from the threshold elevation criterion. This shows that the threshold curvature algorithm correctly identifies small channels but fails to recognize the relatively flat (and wide) bottom of the larger channels.

By combining the threshold elevation and the threshold curvature criteria, we were able to obtain accurate tidal channel network delineation. We obtained the final values of the geomorphic thresholds as follows. First, we plotted the hypsometric curve of the tidal basin (i.e., total basin area below a given elevation versus elevation) in order to note the elevation above which there is a rapid increase in area with minor elevation change (Figure 7a). This elevation delineates the approximate lower height of the marsh plain. We made a similar plot for curvature (Figure 7b). The first estimate of combined values of elevation and curvature was picked near the curve inflections, and then the fine-tuned values were obtained by trial and error comparing the simulated with the observed patterns (Figure 8b). The resulting structure, obtained by employing $z_{cr} = -1.25$ m and $\nabla^2 z_{\text{crit}} = 10^{-3}$ m^{-1}, is shown in Figure 8a.

Indeed, the mixed criterion combines the ability to identify small incisions and channel initiation with the correct attribution of deep, flat zones to the channel network. This analysis was performed across the entire northern lagoon of Venice where the grid sizes of the DTM and of the SPOT field coincide. Nearly 80% of channelized pixels match those extracted from SPOT imagery. Most of the differences occurred in the small channels where uncertainty of alignment of the two grids was particularly important, a common problem in comparing gridded data sets of different origin. Some of the error also stems from imperfect connectivity of the channelized pixels. To improve the connectivity of the tips of the extracted networks (no a priori requirement of connection among channeled sites is postulated by our method), we have checked for isolated channelized sites within a reach comparable with local branch lengths, as briefly described in the Appendix. Other methods to test and improve connectivity, based, for example, on lag-dependent probabilities that channelized pixels at the given lag are connected [e.g., *Allard and Group*, 1993], are being tested and will be described elsewhere. An example of final reconstruction of a detailed tidal network within the northern Lagoon is shown in Figure 9.

4. Scaling Structure of Tidal Networks

Many variables control the environment where the network develops, first of all, the oscillatory tidal motion but also storm surges and floods, wind waves, availability and quality of sediments, salt marsh vegetation, freshwater effects and, importantly, the anthropic presence. Before discussing the scaling properties of the tidal networks reconstructed in section 3, we will describe briefly some features characterizing a tidal basin to infer sources of or departures from scale invariance.

In a salt marsh the planar configuration of creeks appears to be highly variable (see, e.g., Figure 2). In the upper part of the marsh near dry land, drainage patterns bear strong resemblance to terrestrial drainage systems. Channel sinuosity is low and closed loops are few. On the contrary, in the low salt marshes, that is, approaching tidal flats, meanders are common, leading sometimes to loops and cutoffs. In the tidal case the wavelength of meandering is comparable to the length scale of branching within the network, quite differently from what is observed and predicted for fluvial networks [e.g., *Blondeaux and Seminara*, 1985]. In any case it is clear that the peculiarities of tidal meanders will deserve thorough attention in the future.

The most distinct visual imprinting of tidal networks is the large width of channels compared to their drainage area. It is also interesting that tributaries typically enter at 90° (see, e.g.,

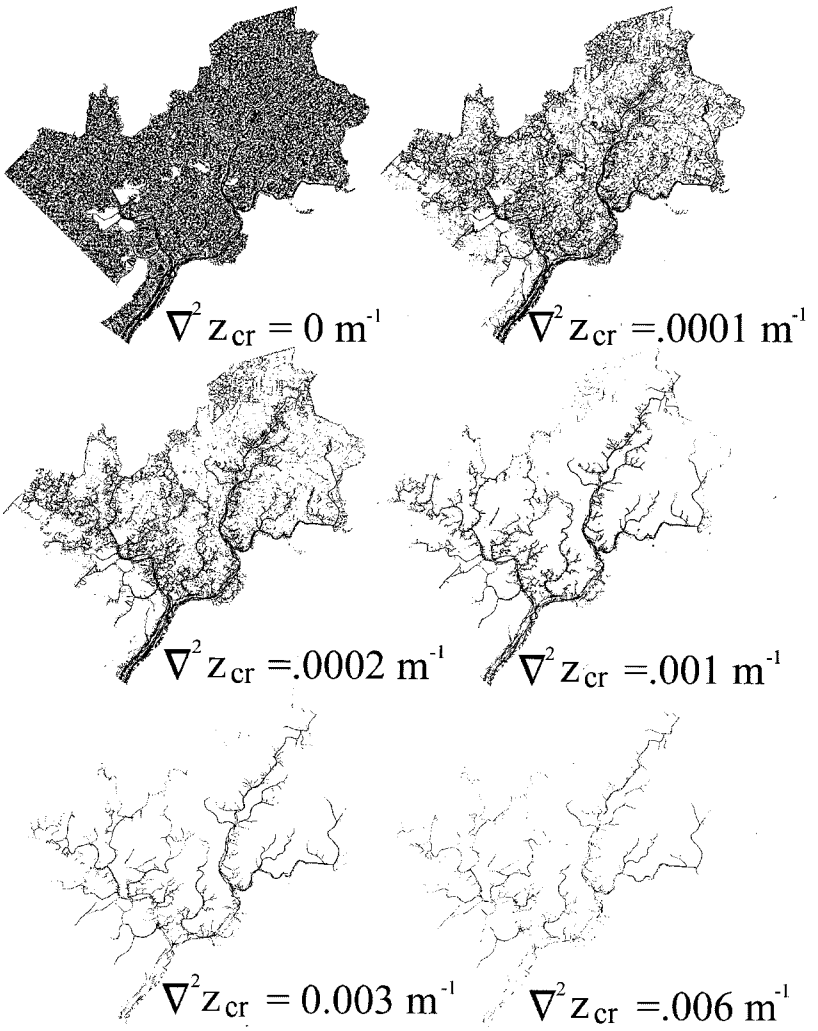

Figure 6. Network structure of the northern part of the Venice Lagoon obtained through the curvature threshold criterion for various values of the threshold: $\nabla^2 z_{cr} = 0.003\ m^{-1}$; $\nabla^2 z_{cr} = 0.006\ m^{-1}$; $\nabla^2 z_{cr} = 0.0002\ m^{-1}$; $\nabla^2 z_{cr} = 0.001\ m^{-1}$; $\nabla^2 z_{cr} = 0.0\ m^{-1}$ (i.e., only topographically concave areas are shown); and $\nabla^2 z_{cr} = 0.0001\ m^{-1}$. Notice that the simple requirement of topographic concavity ($\nabla^2 z \geq 0$) does not yield appreciable landforms.

Figures 2 and 3), a value one would expect for large slope differences between terrestrial tributaries and their mainstream, as, for example, *Howard* [1994] reasoned. To understand similarities and differences with terrestrial systems, one has to realize that marsh tidal networks are strongly influenced by vegetation which stabilizes channel banks thereby controlling channel shape and migration [*Pestrong*, 1965]. In tidal flats, loops and meanders are less frequent. The drainage density appears to be small as well as the link order of channels. Also, tidal flat channels are usually larger and deeper than salt marsh creeks.

Such complex network patterns can be suitably studied by using the tools of fractal geometry extensively adopted in the analysis of river networks (for a review see *Rodriguez-Iturbe and Rinaldo* [1997]). Unlike river networks, however, when considering a tidal network, scaling effects related to finite channel widths (which quite often are comparable with channel length) are likely to play a nonnegligible role. In fact, the scaling behavior of tidal channels not only depends on the manner in which the various branches join together and in the irregularities of individual streams but also on the effect of the upstream narrowing experienced by single channels (as suggested by *Nikora* [1991] in the context of drainage networks). Here the effect is definitely more pronounced than in the fluvial case. One might argue, in fact, that the most striking difference with fluvial networks lies in the larger portion of the available area occupied by channel cross section and the larger spatial gradients of channel widths. We suggest that the characterization of tidal channels is best addressed within the context of nonnegligible transverse channel dimensions, that is, the context of "fat" fractals. Within this framework, which has been previously used, for example, by *Karlinger and Troutman* [1992] to study the properties of spatial networks generated by a random network model, one analyzes the set obtained by subtracting the channeled area (i.e., the total number of the pixels attributed to the tidal channels via the automatic procedure described in section 3) from the total drainage area and replacing the finite channel width with the trace of its centerline pixel (or, equivalently, by the line obtained by joining the

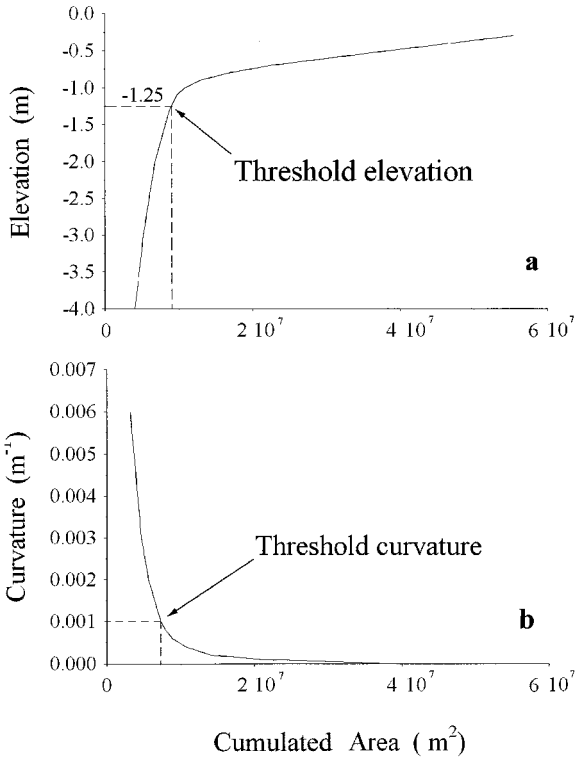

Figure 7. Identification of the geomorphic thresholds for tidal channelization: (a) elevation threshold deduced by the rates of change of the hypsometric curve and (b) proportion of basin area characterized by a given curvature. In both plots the final values chosen for network extraction are shown.

centers of circles inscribed into the channel, see the Appendix) [*Eykholt and Umberger*, 1988].

We first describe a traditional fractal analysis of the channel network regardless of the effects of the actual channel width. In this case the (thin) set of channelized pixels is covered by "boxes" of varying size according to the usual box-counting procedure [*Mandelbrot*, 1982], through which the dimension δ of the set is given by

$$\delta = \lim_{\varepsilon \to 0} \frac{\log N(\varepsilon)}{\log \varepsilon}, \tag{1}$$

where ε is the box-counting grid resolution and $N(\varepsilon)$ is the number of boxes covering the tree-like structure at the resolution ε, obtained by counting the channelized pixels at that resolution.

The computational procedure consists of producing log-log plots of the number of boxes covering the network $N(\varepsilon)$ versus different box bins ε (Figure 10). On coarse graining (i.e., widening the box size and deciding whether the larger box is channelized or not by a predefined rule) the rule adopted is to assign the coarse-grained pixel of size $\varepsilon' > \varepsilon$ to the channelized set when it contains at least one pixel which is channelized at resolution ε.

Figure 10 shows the results of the analyses carried out on some typical creek networks in the Venice Lagoon, in the Petaluma salt marsh, and in Barnstable great marsh. Figure 10a shows the results of the box-counting analysis carried out by considering only the skeleton (Appendix) of the creek network of the Pagliaga salt marsh in the Venice Lagoon extracted from 1×1 m^2 DTM, which filters out the effects of channel widths and addresses the features of total channel lengths. The creek skeleton [*Sagar*, 1996] is defined as the set of the centers of the largest circles that may be inscribed in the channel network (Appendix). The experimental data in Figure 10a fall on two straight lines with a fairly good approximation. The first line, characterizing the larger grid sizes, has a negative slope of nearly 1.7, while the second regime, typical of small grid sizes, has a slope close to -1 thus implying that at small scales ($\varepsilon \to 0$) the skeleton network has a vanishing measure characteristic of a line. The trend exhibited by the experimental values in Figure 10a is confirmed by those shown in Figures 10b and 10c, referring to the skeleton of two typical creek networks in Petaluma Marsh and in Barnstable great marsh, respectively. The departure from a straight line (especially in the Petaluma Marsh) exhibited by data corresponding to larger values of ε is dependent on the size of the salt marsh area analyzed. The

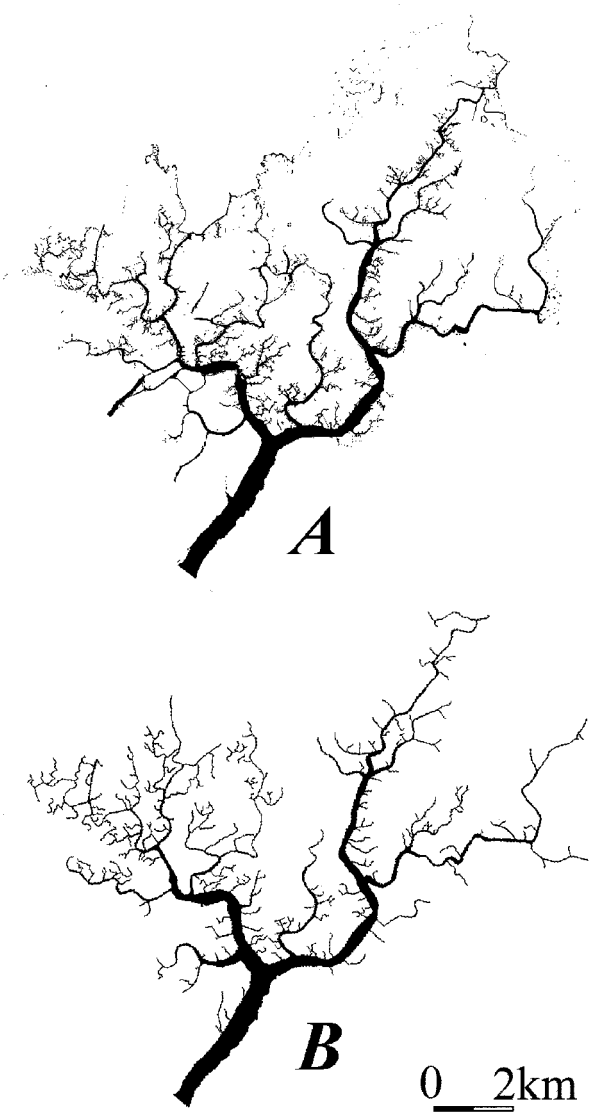

Figure 8. Comparison between network structures of the northern part of the Venice Lagoon, (a) reconstructed from bathymetric data using the combined threshold criterion ($z_{cr} = -1.3$ m and $\nabla^2 z_{cr} = 0.001$ m^{-1}) and (b) identified from manual manipulation of satellite imaging.

relatively small spatial dimensions of the salt marshes and the difficulty of finding relatively large undisturbed marsh areas reduce the observable scale-invariant behavior to roughly two log cycles. The box-counting analysis carried out for the skeleton of the whole northern part of the Venice Lagoon is shown in Figure 10d. The higher slope of the straight line characterizing larger ε (-1.5 instead of -1.7) suggests that the scaling properties of channel networks in tidal flats differ from those of salt marshes, a result consistent with intuition (see also J. Cleveringa and A. P. Oost, The fractal geometry of tidal-channel systems in the Dutch Wadden Sea, preprint *Geologie en Mijnbouw*, 1997). In contrast to the salt marsh some parts of tidal flats lack channels or a branching network (see, e.g., Figure 2), and the dynamical reason for this is unclear.

Interesting facts emerge. The break in the scaling relationship for different planar patterns of tidal networks (the detailed planar map of Palude Pagliaga (1×1 m^2), Petaluma, Barnstable marshes, and the entire Venice Lagoon (20×20 m^2)) suggests the usual transition from global to local fractal dimensions [see, e.g., *Rodriguez-Iturbe and Rinaldo*, 1997, chapter 2]; the former is dominated by the sinuosity of individual channels; the latter is dominated by the branching properties of the network. The fact that the length scale ε at which we observe the break varies considerably (even (Figures 10a and 10d) within the same tidal basin) shows a definite nonuniversal behavior regardless of finite-width effects. Moreover, the scale at which we observe the break is generally too large to argue some influence of the inappropriate definition of the fine structure of the network. The difference in the transition scale from global to local scaling in Figure 10 does not seem to depend on different resolutions. Different transitions may be attributed to spatially inhomogeneous branching structures detected by our method where we observe large differences in drainage density [see *Rinaldo et al*., this issue (a)]. Moreover, it is not clear how the finite-size width affects the above scaling for large sizes.

A scaling analysis accounting for the finite size of the channel width has also been addressed, following the work of *Karlinger and Troutman* [1992]. We have considered the properties of the set defined by the portion of the tidal basin not occupied by channels. Owing to finite channel width this is a set with fractal boundaries [*Eykholt and Umberger*, 1988]. As in the case of the dimension in (1), different scaling exponents can be defined through a coarse-graining procedure similar to that

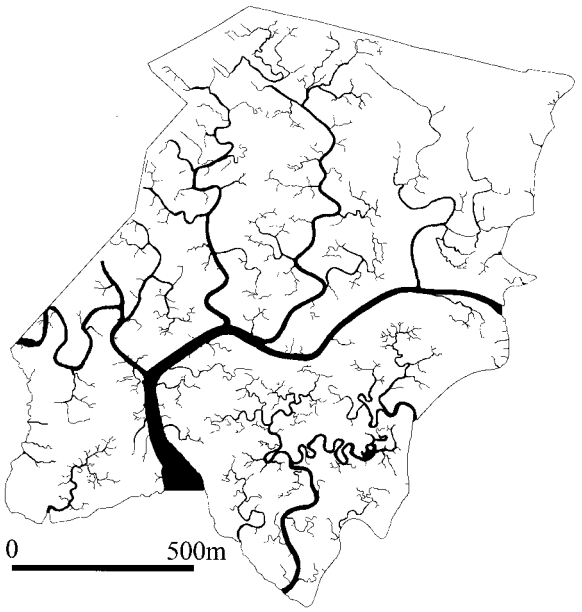

Figure 9. Creek network within the Palude Pagliaga Marsh identified from combined aerial photographs and bathymetries.

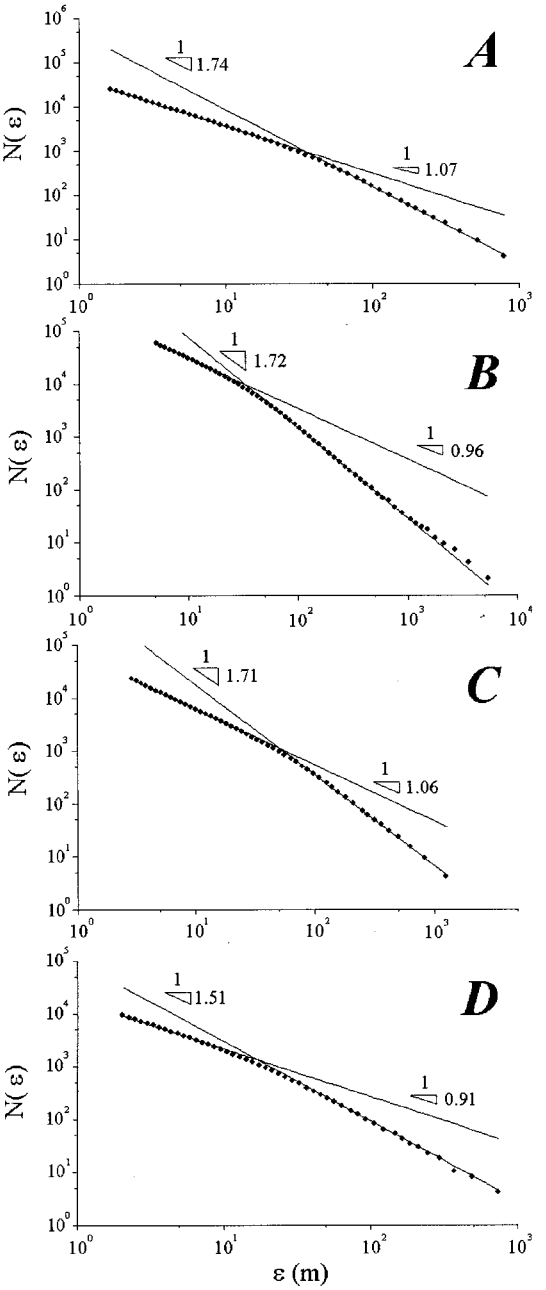

Figure 10. Box-counting analysis as in equation (1) applied to (a) a tidal creek network within the Pagliaga salt marsh (Venice) (1×1 m^2 grid size), analyzed by considering only the skeleton (Appendix) of the network; (b) the skeleton of the tidal network within Petaluma Marsh; (c) the skeleton of the tidal network within Barnstable great marsh (Massachusetts); and (d) the entire skeleton of the tidal networks of the northern part of the Venice Lagoon.

described above. The "fat" fractal exponent, say γ, is defined by

$$\gamma = \lim_{\varepsilon \to 0} \frac{\log|\varepsilon^D N(\varepsilon) - \mu_0|}{\log \varepsilon}, \tag{2}$$

where ε is the box-counting grid resolution, D is the dimension of the embedding space (here $D = 2$), $N(\varepsilon)$ is the number of boxes containing part of the fat fractal set defined above, and μ_0 denotes the finite asymptotic value of the area of the set in the limit as $\varepsilon \to 0$. For any set, γ varies in the range $0 \leq \gamma \leq D$. For a "thin" fractal set $\mu_0 = 0$ the exponent γ represents the codimension of the boundary of the set, which is linked to δ in (1) by the relationship $\delta = D - \gamma$ [*Grebogi et al*., 1985]. This is not generally the case, however, for fat fractals [*Eykholt and Umberger*, 1988]. In the fractal jargon, channelized sets reduced to their skeletons (Appendix) are said to have zero Lebesgue measure.

In order to capture the scaling characters of the areal properties of the channel planform and owing to the reported difficult numerical evaluation of μ_0 in (2) [*Troutman and Karlinger*, 1992], a related scaling exponent, say β, is best introduced. The exponent controls the rate of change of planform areas occupied by the network and is defined as [*Eykholt and Umberger*, 1988]

$$\beta = \lim_{w \to 0} \frac{\log A(\leq w)}{\log w}, \tag{3}$$

where w is the channel width, measured in meters (related computational aspects are described in the Appendix), and $A(\leq w)$ is the area (square meters) occupied in plan by tidal streams whose width is less than or equal to a chosen value w. By varying the values of w, (3) allows the computation of the exponent β ($0 \leq \beta \leq \infty$) which characterizes the relative importance, in terms of areal extension, of channel structures of different scales. The larger the values of β are, the more prominent the features of subsets of the overall network characterized by large widths with respect to the finer structures are. It can also be shown that the above coefficients are related [*Eykholt and Umberger*, 1988, 1992]. For any bounded set in any number of dimensions, β is related to γ by the relationship $\gamma = \beta$, with $\beta \leq 1$ and $\gamma = 1$ for $\beta > 1$. Hence the fat fractal set is derived from the set previously defined essentially by considering the scaling properties of salt marsh areas minus the surface area of creeks.

Figures 11a–11d illustrate the function $A(\leq w)$ plotted versus the width w in a double logarithmic plot for the three different salt marsh environments considered above, namely, the finely measured Palude Pagliaga salt marsh (Venice), Petaluma Marsh and Barnstable great marsh, and the overall northern lagoon of Venice measured at a coarser level of detail.

Noteworthy differences among the analyzed sets are observed. In three out of four cases the function A shows a rather sharp break in the area-width relationship, suggesting that the rates of change of widths are significantly modified. Of course, the procedure is coarse and global and thus unable to distinguish why the departure occurs at different widths for the three environments studied in this paper. One possible explanation, addressed in a companion paper [*Rinaldo et al*., this issue (b)] relates to the transition from ebb-dominated to flood-dominated hydrodynamics, that is, whether the landscape-forming flow rates are produced in ebb or flood conditions.

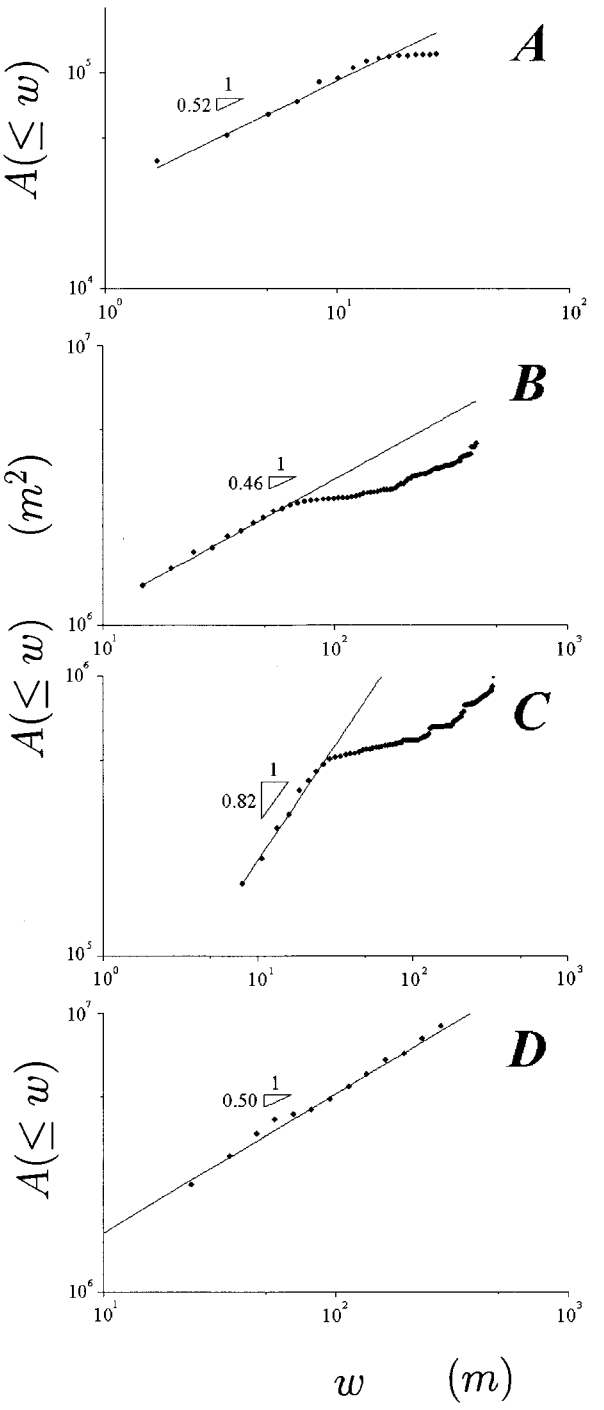

Figure 11. Fat fractal analysis, that is, scaling of the function $A(\leq w)$ versus w as discussed in equation (3). The analysis is applied to (a) tidal networks within the Pagliaga salt marsh (Venice); (b) the tidal network of Petaluma Marsh; (c) the Barnstable great marsh; and (d) the entire structure of tidal channel networks within the northern part of the Venice lagoon. Notice the important breaks in the scaling relationships.

This condition occurs because of asymmetries induced in the tidal propagation within complex embayments cut by deep networks. Topographic factors, for example, the average elevation of unchanneled areas, or hydrodynamic factors like tidal amplitudes (which, coupled with topography, determine the

spatial gradients of flow rates) may also play a distinctive role in different sites. It seems reasonable, however, that the chief geomorphic processes strongly depend on local conditions for tidal networks differently from the fluvial case, although any conclusion at this stage would be premature. Here it suffices to show the potential of the proposed method for an exhaustive study.

An exponent β has been fitted merely to distinguish the trends shown by the data, although the spatial ranges are far too limited to suggest any scaling insight. The estimated values of β are 0.52, 0.46, 0.82, and 0.50, for Figures 11a–11d, respectively. Overall, such values imply that the occupied area changes significantly with channel widths. The lowest value of β pertains to the Petaluma Marsh, whose channel network appears to be characterized by large and uneven drainage density (Figure 3). The differences among the values of β, reflecting vastly different hydrodynamics and topographic and environmental conditions, are noteworthy. These differences suggest a major distinction between tidal channels and river networks, the latter showing small differences overall in fractal attributes. Furthermore, the fact that $\beta < 1$ implies $\beta = \gamma$ [*Eykholt and Umberger*, 1992], suggesting that both small- and large-scale structures contribute to the fractal properties of the set. The discrepancy between the exterior dimension $\delta = 2 - \gamma$ [*Grebogi et al*., 1985] of the boundary of the fat fractal set (the creek network) and a rough estimate of the thin fractal dimension ($\delta \sim -1.7$) inferred from Figures 10a–10c agrees with previous results [*Eykholt and Umberger*, 1988] which established that an equality need hold only for thin fractal sets.

We finally note that no break in relationship (3) is observed for the entire range of values of w for the northern part of the Venice Lagoon measured on the coarse grid (Figure 11d). Whether this is an artifact of the coarse grid or the signal of lack of transition from one leading landscape-forming mechanism to another remains to be seen (see, for a preliminary account, *Rinaldo et al*. [this issue (a)].

5. Conclusions

We have proposed a methodology for the automatic extraction of tidal networks from digital terrains of tidal basins that may include salt marshes as well as tidal flats. Our criterion, which is based on the joint exceedence of a critical depth and of a critical curvature in areas characterized by topographic concavity, yields channelized patterns in tidal areas matching well network delineation through digital imaging. From our analysis and from previously published data on tidal networks, we conclude that channel networks in different tidal basins exhibit quite different overall scaling characteristics, depending on the particular areas considered. This contrasts markedly with the relative small range of scaling attributes in river networks. Given the diversity of the relevant dynamics (discussed by *Rinaldo et al*. [this issue (a)], this is not surprising. Nevertheless, the network skeletons in the salt marshes have box-counting dimensions of about 1.7, suggesting some similarity and weak distinctiveness of the box-counting attributes. The strongest departure from fractal characters occurs near the inlet where the penetration of channels cutting into the basin is much weaker than that of creeks within a salt marsh.

We have also found that tidal networks can be conveniently analyzed through the fat-fractal formalism owing to nonnegligible widths of the channels with respect to the basin length scale. "Fat" scaling exponents prove consistently lower than unity and differ substantially from site to site.

Appendix

In this Appendix we discuss technical details on the automatic, and thus objective, determination of important geometrical features like the base width of an arbitrarily oriented rooted tree or the geometric coordinates of its skeleton.

We first outline the algorithm devised to compute the point-by-point widths of the branching tidal channels. Let $\mathcal{D}$ be a set of labeled pixels in a regular grid (Figure A1a). In our case, labeling the pixels indicates their belonging to the tree structures (i.e., the channelized portion of the tidal landscape, see section 2) we intend to analyze. Let us define for every pixel (i.e., point) of $\mathcal{D}$ a quantity w called width as follows: For every pixel of the set the width w is defined as the maximum diameter of all the circles that can be inscribed in the set including the pixel. Notice that a circle is inscribed in the set if every pixel inside the circle actually belongs to the set (Figure A2). Thus the arbitrary pixel does not necessarily coincide with the center of the maximum circle.

When applied to a channel network, the above definition enables us to find the width of every channel and to characterize this quantity even in branching zones. We have devised a novel algorithm to numerically compute the set of all channel widths of an arbitrary tree. We start with the set $\mathcal{D}$ (Figure A1a). An arbitrary length r is assumed. The first step is to delete from the set all the sites characterized by distance less

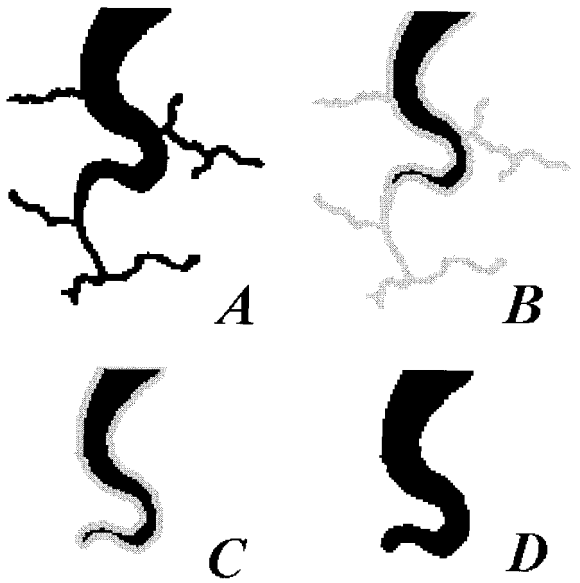

Figure A1. An illustration of the four-step algorithm designed to identify the widths of a set of points. When applied to a channel network, the above definition enables us to find the width of every channel and to characterize this quantity even in branching zones. (a) Set of channelized pixels. (b) The first step of deleting from the set all the sites characterized by distance less than a fixed distance r from a point outside the set (shaded pixels). (c) The expanded set obtained by thickening it by adding every adjacent pixel (solid plus shaded pixels). (d) A new set defined. This set has two properties: every point of Figure A1d belongs to Figure A1a, and (by construction) it is the union set of all the circles with radius r inscribed in the set.

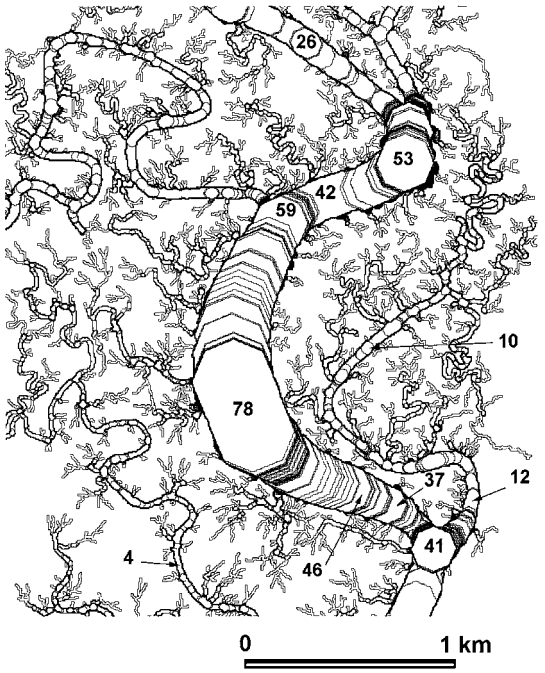

Figure A2. Automatic computation of the widths of a tidal channel network. The numbers represent the radius of the maximum circles inscribed in the channels. Notice that the procedure is of general nature and applies to any digital terrain maps (DTMs) where the size of the pixel is significantly smaller that channel widths. We expect, for instance, this to occur in terrestrial DTMs where laser-borne altimetries are used.

than r from a point outside the set (the shaded pixels in Figure A1b). It can be shown that the set $\mathcal{C}_r$ of the remaining pixels (solid in Figure A1b) represents the centers of all the possible circles of radius r inscribed in the set $\mathcal{D}$. Now we expand the set $\mathcal{C}_r$ thickening it by adding every adjacent pixel (i.e., whose distance is less than r from any point of the set $\mathcal{C}_r$). Actually, one just needs to add only the pixels distant less than r from the boundary of the set $\mathcal{C}_r$ (solid plus shaded pixels in Figure A1c). In this manner we define a new set $\mathcal{W}_r$ (solid in Figure A1d). This set has two properties: Every point of $\mathcal{W}_r$ belongs to $\mathcal{D}$; (by construction) $\mathcal{W}_r$ is the union set of all the circles with radius r inscribed in the set.

On changing the length r, we obtain a family of sets $\mathcal{W}_r$ depending on the radius r of the circles inscribed. The last step yields the definition of w for a pixel, say P,

$$w = 2 \max \{r : P \in \mathcal{W}_r\}; \tag{A1}$$

that is, w is twice the maximum radius r belonging to the set $\mathcal{W}_r$ that contains the pixel P.

Figure A2 shows the result of the application of this algorithm for a tidal channel network. Within our square lattice the circles are suitably approximated by octagons. Technically, an octagon of radius $\sqrt{2}$ is constructed through the outer sides of the nearest neighbors (in coordinate directions) to the center pixel and the diagonals joining the vertices for the remaining (diagonal) pixels.

We now turn to the algorithmic definition of the skeleton of a connected set of pixels. Using an algorithm similar to the previous one, it is possible to find, for every branch of channel, its skeleton, that is, the median line. The skeleton of a channel is defined as the line joining the centers of the maximum circles that can be inscribed in the network. A property of these circles is that they touch the boundary of the channels in two points. Following this approach and after having chosen a value r, we first delete from the set (Figure A3a) every point whose distance from the boundary is less than r, finding the set, say, $\mathcal{C}_r$ (Figure A3b). The same algorithm is applied to the same set, deleting the points at distance $r + 1$ and finding a new set $\mathcal{C}_{r+1}$. We then sum to $\mathcal{C}_r$ all the sites with distance less than 1. The resulting set is $\mathcal{W}_{r+1}$ (Figure A3c). The points belonging to $\mathcal{C}_r$ but not to $\mathcal{W}_{r+1}$ have the following property: They belong to $\mathcal{C}_r$, so they are centers of circles of radius r inscribed into the channels, yet they do not belong to $\mathcal{W}_{r+1}$, so they are not included in circles of radius $r + 1$. In other words, one cannot inscribe a circle of radius larger than r through these points, that is, the points are centers of circles with maximum radius, and so they belong to the skeleton. Repeating the analysis for every r, we identify all the centers of the maximum circles inscribed in the channels. This set of centers is called the skeleton (Figure A4). Notice that at confluences the skeleton is discontinuous, so that the main backbone and the smaller branches issuing from it are not necessarily connected.

We now address the identification of the sections of a tidal channel. In geomorphological studies of tidal channel networks it is of crucial importance to estimate, in some automatic manner, the channel cross sections. In a two-dimensional planar representation of the network the cross sections of every channel become linear segments which cut the channels per-

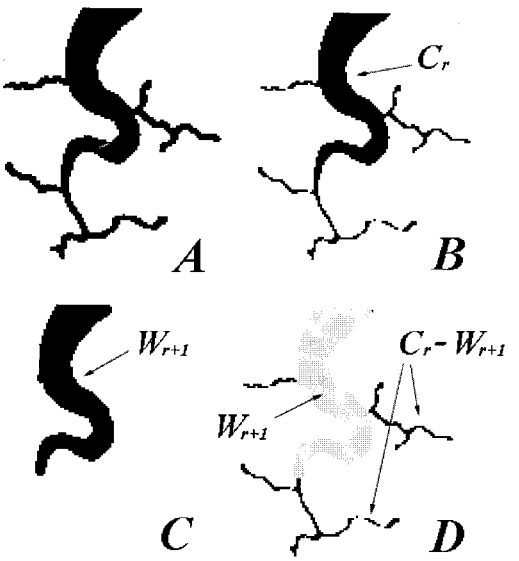

Figure A3. An illustration of the four-step algorithm designed to identify the skeleton of a connected set of pixels. We now turn to the algorithmic definition of the skeleton of a connected set of pixels. Using an algorithm similar to the one illustrated in Figure A1, it is possible to find, for every branch of channel, its skeleton, that is, the median line. The skeleton of a channel is defined as the line joining the centers of the maximum circles that can be inscribed in the network. A property of these circles is that they touch the boundary of the channels in two points. (a) The set of channelized pixels. (b) The set of channelized pixels where every point whose distance from the boundary is less than r has been deleted. (c) The same algorithm applied to Figure A3b deleting the points at distance $(r + 1)$. (d) All the sites with distance less than unity added to Figure A3c.

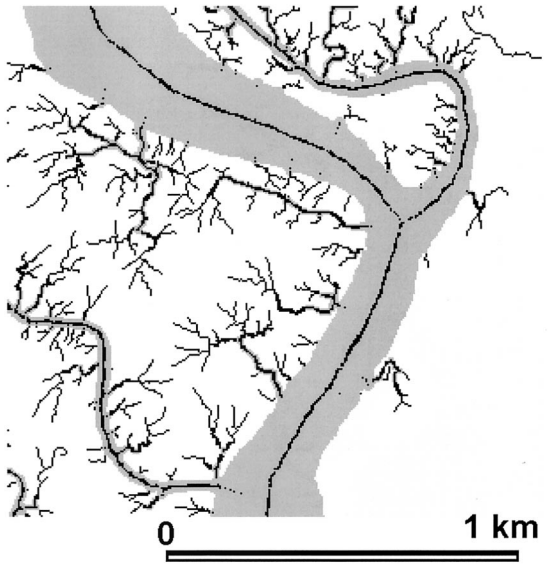

Figure A4. Detail of skeleton for a tidal channel network. The skeleton is the pattern that connecting the centerlines of the inscribed circles whose diameter is the local channel's width.

pendicularly to the banks or sides. Notice that issuing the normal vector to the sides of the channels is not a trivial task, especially at branching points. We now propose an algorithm able to find in a quite precise manner the cross sections and at the same time to calculate the distance of every section from a base of the rooted tree, that is, the tidal inlet.

Figure A5. Cross sections of a tidal channel network: an illustration of the algorithm for automatic extraction of the width. Notice the difficult estimation of widths at major junctions.

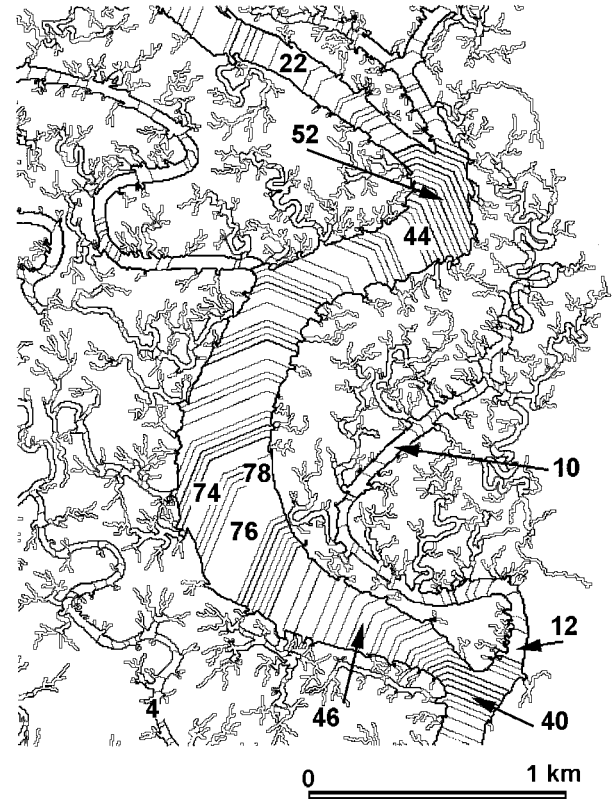

Figure A6. Systematic estimation of cross-section widths of a tidal channel network.

We start from an inlet section. From this section we move one pixel upstream and find for every point the minimum distance from the inlet. The minimum distance from the inlet requires some reasoning, because the algorithm calculates the minimum distance which, within bends of large channels, would not proceed along the median. Nevertheless, in a relatively long tidal channel (in which the length is much larger than the width) this algorithm yields a good approximation of the distance from the inlet. We define as a cross section every set of connected pixels whose distance x from the inlet lies in the interval $d < x \leq d + k$. Through the parameters d and k it is possible to vary the number of pixels belonging to every section (Figure A5).

Finally, the previous definition of width, even if applicable to a more general set of points, has been modified as follows. In a tidal channel it is important to define the width of every section of channel, while the general algorithm yields a different value for every point belonging to the channels. A simple way to yield a single width is to consider the point of the skeleton which belongs to the section. From these points one searches the maximum radius to inscribe a circle which is assumed as the width (Figure A6).

Acknowledgments. The writers thank Consorzio Venezia Nuova (Venice, Italy) for providing the topographic data and some of the aerial images used in this study. Special thanks have to be expressed to P. Baschieri, G. Cecconi, and R. Rosselli (Consorzio Venezia Nuova) for providing topographic data and for interesting discussions. SPOT images have been provided by CNR—Istituto per lo Studio della Dinamica delle Grandi Masse through the courtesy of P. Alberotanza. We also thank P. Baggio and G. Sigalotti (CNR—Universitá di

Padova) for the help provided in image processing and the interesting discussions and J. Collins and R. Grossinger, San Francisco Estuary Institute, for providing valuable information on Petaluma marsh environment and history. We are much indebted to Chris Paola and to an anonymous reviewer for very valuable insight and their constructive criticism on a draft of this paper. Funds provided by MURST (40%) and Universitá di Padova, through the projects Morfodinamica fluviale e costiera and Trasporto di sedimenti ed evoluzione morfologica di corsi d'acqua, estuari e lagune alle diverse scale temporali, are gratefully acknowledged.

References

Adami, A., G. Biotto, and N. Casalini, Ricerca statistica sulla morfologia dei canali lagunari, in *Atti del XX Convegno di Idraulica e Costruzioni Idrauliche*, pp. 1–10, Ed. Libr. Progetto, Padua, Italy, 1986.

Allard, D., and H. Group, On the connectivity of two random set models: The truncated Gaussian and the Boolean, in *Geostatistics Troia 92*, pp. 467–478, Kluwer Acad., Norwell, Mass., 1993.

Allen, J. R. L., and K. Pye, *Salt Marshes*, Cambridge Univ. Press, New York, 1992.

Ashley, G. M., and M. L. Zeff, Tidal channel classification for a low-mesotidal salt marsh, *Mar. Geol.*, *82*, 17–32, 1988.

Ayles, C. P., and M. F. Lapointe, Downvalley gradients in flow patterns, sediment transport and channel morphology in a small macrotidal estuary: Dipper Harbour Creek, New Brunswick, Canada, *Earth Surf. Processes Landforms*, *21*, 829–842, 1996.

Bayliss-Smith, T. P., R. Healey, R. Lailey, T. Spencer, and D. R. Stoddart, Tidal flows in salt-marsh creeks, *Estuarine Coastal Mar. Sci.*, *9*, 235–255, 1979.

Blondeaux, P., and G. Seminara, A unified bar-bend theory of river meanders, *J. Fluid Mech.*, *157*, 449–470, 1985.

Boon, J. D., III, Tidal discharge asymmetry in a salt marsh drainage system, *Limnol. Oceanogr.*, *20*, 71–80, 1975.

Bridges, P. H., and M. R. Leeder, Sedimentary model for intertidal mudflat channels, with examples from the Solway Firth, Scotland, *Sedimentology*, *23*, 533–552, 1976.

Chapman, V. J., *Salt Marshes and Salt Deserts of the World*, Wiley-Interscience, New York, 1960.

Collins, L. M., J. M. Collins, and L. B. Leopold, Geomorphic processes of an estuarine marsh: preliminary results and hypothesis, in *International Geomorphology 1986: Proceedings of the First International Conference on Geomorphology*, vol. 1, edited by V. Gardiner, pp. 1049–1071, John Wiley, New York, 1987.

Comune di Venezia, Previsioni delle altezze di marea per il bacino di S. Marco e delle velocita' di corrente per il Canal Porto di Lido—Laguna di Venezia: Valori astonomici, technical report, 181 pp., Ist. Poligr. dello Stato, Rome, 1997.

Dedrick, K. G., Use of the early hydrographic surveys in studies of California estuaries, in *Coastal Zone '83*, *Coastal and Ocean Management*, *Publ. 3*, pp. 2294–2316, Am. Soc. of Civ. Eng., Reston, Va., 1983.

Dorigo, W., *Venezia Origini*, Electa, Venezia, 1983.

Dronkers, J. J., *Tidal Computations in Rivers and Coastal Waters*, North-Holland, New York, 1964.

Eykholt, R., and D. K. Umberger, Relating the various scaling exponents used to characterize fat fractals in nonlinear dynamical systems, *Physica D*, *30*, 43–60, 1988.

Eykholt, R., and D. K. Umberger, Extension of the fat-fractal exponent β to arbitrary sets in D dimensions, *Phys. Lett. A*, *163*, 409–414, 1992.

French, J. R., and D. R. Stoddart, Hydrodynamics of salt marsh creek systems: Implications for marsh morphological development and material exchange, *Earth Surf. Processes Landforms*, *17*, 235–252, 1992.

Gottardo, D., and S. Cavazzoni, Osservazioni sulla propagazione della marea nella Laguna di Venezia, Rapporti e Studi, *Atti Ist. Veneto Sci. Lett. Arti Cl. Sci. Fis. Mat. Nat.*, *VIII*, 30–37, 1981.

Grebogi, C., S. W. McDonald, E. Ott, and J. A. Yorke, Exterior dimension of fat fractals, *Phys. Lett. A*, *110*, 1–4, 1985.

Grossinger, R. M., Historical evidence of freshwater effects on the plan form of tidal marshlands in the Golden Gate Estuary, Master thesis, Univ. of Calif., Santa Cruz, 1995.

Healey, R. G., K. Pye, D. R. Stoddart, and T. P. Bayliss-Smith, Velocity variation in salt marsh creeks, Norfolk, England, *Estuarine Coastal Shelf Sci.*, *13*, 535–545, 1981.

Horton, R. E., Erosional development of streams and their drainage basins: Hydrophysical approach to quantitative geomorphology, *Geol. Soc. Am. Bull.*, *56*, 275–370, 1945.

Howard, A. D., A detachment-limited model of drainage basin evolution, *Water Resour. Res.*, *30*(7), 2261–2285, 1994.

Jacobson, H. A., Historical development of the salt marsh at Wells, Maine, *Earth Surf. Processes Landforms*, *13*, 475–486, 1988.

Karlinger, M. R., and B. M. Troutman, Fat fractal scaling of drainage networks from a random spatial network model, *Water Resour. Res.*, *28*(7), 1975–1981, 1992.

Kirchner, J. W., Statistical inevitability of Horton's laws and the apparent randomness of stream channel networks, *Geology*, *21*, 591–599, 1993.

Knighton, A. D., C. D. Woodroffe, and K. Mills, The evolution of tidal creek networks, Mary River, northern Australia, *Earth Surf. Processes Landforms*, *17*, 167–190, 1992.

Leopold, L. B., and T. Maddock, Jr., The hydraulic geometry of stream channels and some physiographic implications, *U. S. Geol. Surv. Prof. Pap.*, *252*, 56 pp., 1953.

Leopold, L. B., L. Collins, and M. Inbar, Channel and flow relationships in tidal salt marsh wetlands, *Tech. Rep. G830-06*, 78 pp., Calif. Water Resour. Cent., U. S. Geol. Surv. Davis, 1984.

Leopold, L. B., J. N. Collins, and L. M. Collins, Hydrology of some tidal channels in estuarine marshlands near San Francisco, *Catena*, *20*, 469–493, 1993.

Mandelbrot, B. B., *The Fractal Geometry of Nature*, W. H. Freeman, New York, 1982.

Montgomery, D. R., and W. E. Dietrich, Where do channels begin?, *Nature*, *336*, 232–234, 1988.

Montgomery, D. R., and W. E. Dietrich, Channel initiation and the problem of landscape scale, *Science*, *255*, 826–830, 1992.

Montgomery, D. R., and E. Foufoula-Georgiou, Channel network source representation using digital elevation models, *Water Resour. Res.*, *29*(12), 1925–1934, 1993.

Myrick, R. M., and L. B. Leopold, Hydraulic geometry of a small tidal estuary, *U. S. Geol. Surv. Prof. Pap.*, *422-B*, 18 pp., 1963.

Nikora, V. I., Fractal structures of river plan forms, *Water Resour. Res.*, *27*(6), 1327–1333, 1991.

Pestrong, R., The development of drainage patterns on tidal marshes, *Stanford Univ. Publ. Geol. Sci.*, *10*, 87 pp., 1965.

Redfield, A. C., Development of a New England salt marsh, *Ecol. Monogr.*, *24*, 2, 201–237, 1972.

Rinaldo, A., I. Rodriguez-Iturbe, and R. Rigon, Channel networks, *Annu. Rev. Earth Planet. Sci.*, *26*, 289–327, 1998.

Rinaldo, A., S. Fagherazzi, S. Lanzoni, M. Marani, and W. E. Dietrich, Tidal networks, 2, Watershed delineation and comparative network morphology, *Water Resour. Res.*, this issue (a).

Rinaldo, A., S. Fagherazzi, S. Lanzoni, M. Marani, and W. E. Dietrich, Tidal networks, 3, Landscape-forming discharges and studies in empirical geomorphic relationships, *Water Resour. Res.*, this issue (b).

Rodriguez-Iturbe, I., and A. Rinaldo, *Fractal River Basins: Chance and Self-Organization*, Cambridge Univ. Press, New York, 1997.

Sagar, B. S. D., Fractal relation of a morphological skeleton, *Chaos Solitons Fractals*, *7*(11), 1871–1879, 1996.

Shi, Z., H. F. Lamb, and R. L. Collin, Geomorphic change of salt marsh tidal creek networks in the Dyfi Estuary, Wales, *Mar. Geol.*, *128*, 73–83, 1995.

van Straaten, L. M. J. U., Composition and structure of recent marine sediments in the Netherlands, *Leidse Geol. Meded.*, *19*, 1–110, 1954.

Woldenberg, M., Relations between Horton's laws and hydraulic geometry as applied to tidal networks, *Harvard Pap. Theor. Geogr.*, *45*, 1–39, 1972.

A. Adami, S. Lanzoni, M. Marani, and A. Rinaldo, Dipartimento di Ingegneria Idraulica, Marittima e Geotecnia, Universitá di Padova, via Loredan 20, I-35131 Padua, Italy. (adami@idra.unipd.it; lanzo@idra.unipd.it; marani@idra.unipd.it; rinaldo@idra.unipd.it)

A. Bortoluzzi, PROTECNO, via dei Colli, 131 Padua, Italy.

W. E. Dietrich, Department of Geology and Geophysics, University of California, Berkeley, Berkeley, CA 94720. (bill@geomorph.berkeley.edu)

S. Fagherazzi, Computational Science and Engineering Program, Florida State University, Tallahassee, FL 32306. (sergio@cse.fsu.edu)

(Received August 5, 1998; revised July 16, 1999;
accepted July 21, 1999.)